pensate for a deficiency of GATA-1 during erythroid development. Gene targeting should also be useful in delineating the individual developmental functions of other transcription factors with potential redundancy, such as the multiple octamer-binding proteins[24].

Although most autosomal recessive mutations produced in ES cells must be bred to homozygosity before any phenotypic effects are evident[25,26], the fact that male cells are hemizygous for the X-linked GATA-1 gene has enabled us to examine the consequences of a targeted mutation through the direct analysis of chimaeric mice. If mutant ES cells can contribute to the germ line in viable chimaeric males, it will be interesting to follow the development of embryos with cells uniformly deficient in GATA-1. Meanwhile we can use chimaeras to provide an answer to questions such as whether this factor is also necessary for the development of primitive, yolk sac-derived erythroid cells, or for the differentiation of megakaryocytes or mast cells. Finally, the mutant ES cells provide a null background in which altered versions of the GATA-1 gene can be introduced to test the effects of directed mutations on erythroid development.

Received 31 August; accepted 29 October 1990.

1. Orkin, S. H. *Cell* **63,** 665–672 (1990).
2. Martin, D. I. K., Tsai, S. -F. & Orkin, S. H. *Nature* **338,** 435–438 (1989).
3. Tsai, S. -F. *et al. Nature* **339,** 446–451 (1989).
4. Wall, L., deBoer, E. & Grosveld, F. *Genes Dev.* **2,** 1089–1100 (1989).
5. Evans, T., Reitman, M. & Felsenfeld, G. *Proc. natn. Acad. Sci. U.S.A.* **85,** 5976–5980 (1988).
6. Evans, T. & Felsenfeld, G. *Cell* **58,** 877–885 (1989).
7. Mignotte, V., Wall, L., deBoer, E., Grosveld, F. & Romeo, P. -H. *Nucleic Acids Res.* **17,** 37–54 (1989).
8. Youssoufian, H., Zon, L., Orkin, S. H., d'Andrea, A. D. & Lodish, H. F. *Molec. cell. Biol.* **10,** 3675–3682 (1990).
9. Brady, H. J. M., Sowden, J. C., Edwards, M., Lowe, N. & Butterworth, P. H. W. *FEBS Lett.* **257,** 451–456 (1989).
10. Reitman, M. & Felsenfeld, G. *Proc. natn. Acad. Sci. U.S.A.* **85,** 6267–6271 (1988).
11. Frampton, J., Walker, M., Plumb, M. & Harrison, P. R. *Molec. cell. Biol.* **10,** 3838–3842 (1990).
12. Martin, D. I. K. & Orkin, S. H. *Genes Dev.* **4,** 1886–1898 (1990).
13. Martin, D. I. K., Zon, L. I., Mutter, G. & Orkin, S. H. *Nature* **344,** 444–447 (1990).
14. Romeo, P. -H. *et al. Nature* **344,** 447–449 (1990).
15. Yamamoto, M. *et al. Genes Dev.* (in the press).
16. Wilson, D. B., Dorfman, D. M. & Orkin, S. H. *Molec. cell. Biol.* **10,** 4854–4862 (1990).
17. Mansour, S. L., Thomas, K. R. & Capecchi, M. R. *Nature* **236,** 438–452 (1988).
18. Robertson, E., Bradley, A., Kuehn, M. & Evans, M. *Nature* **323,** 445–448 (1986).
19. DiChiara, T. M., Efstratiadis, A. & Robertson, E. J. *Nature* **344,** 78–80 (1990).
20. Zon, L. I. *et al. Proc. natn. Acad. Sci. U.S.A.* **87,** 668–672 (1990).
21. Russell, E. S. & McFarland, E. C. *Ann. N.Y. Acad. Sci.* **241,** 25–38 (1974).
22. McCulloch, E. A., Siminovitch, L. & Till, J. E. *Science* **144,** 844–846 (1964).
23. Scholer, H. R., Hatzopoulos, A. K., Balling, R., Suzuki, N. & Gruss, P. *EMBO J.* **8,** 2543–2550 (1989).
24. Fleischman, R. A., Custer, R. P. & Mintz, B. *Cell* **30,** 351–359 (1982).
25. Zijlstra, M. *et al. Nature* **344,** 742–746 (1990).
26. Koller, B. H., Marrack, P., Kappler, J. W. & Smithies, O. *Science* **248,** 1227–1230 (1990).
27. Thomas, K. R. & Capecchi, M. R. *Cell* **51,** 503–512 (1987).
28. Robertson, E. J. in *Teratocarcinomas and Embryonic Stem Cells: A Practical Approach* (ed. Robertson, E. J.) 71–112 (IRL, Oxford, 1987).
29. McLaren, A. & Buehr, M. *Genet. Res. Camb.* **37,** 305–309 (1981).
30. Whitney, J. B. III *Biochem. Genet.* **16,** 667–672 (1978).

ACKNOWLEDGEMENTS. We thank R. M. Young for assistance with plasmid polyoma HSV-tk. This work was supported by grants to F.C. and S.H.O. from the NIH and the ACS. L.P. is a March of Dimes Predoctoral Fellow, S.H.O. is an Investigator and M.C.S. is an Associate of the Howard Hughes Medical Institute, and E.J.R. is a Leukemia Society Scholar.

Ultrastructural basis and function of iridescent blue colour of fruits in *Elaeocarpus*

David W. Lee

Department of Biological Sciences, Florida International University, University Park, Miami, Florida 33199 and Fairchild Tropical Garden, Miami, Florida 33156, USA

IRIDESCENT colour, caused by physical effects (thin-film interference, diffraction and Tyndall scattering), is relatively common in animals but exceedingly rare among plants[1]. Some benthic marine algae produce blue to violet iridescence[2,3], and the upper leaf surfaces of a few vascular plants from the shady environments of humid tropical forests are iridescent blue[4–6]. Blue fruit colour has been assumed to be caused by anthocyanins[7]. A survey of such fruits (26 species in 18 genera) in Costa Rica, India, Florida and Malaysia, showed this to be the case, except for the iridescent colour in fruits of *Elaeocarpus angustifolius* Blume (Elaeocarpaceae). There I show that the colour is caused by a remarkable structure in the epidermis, and provide evidence for its selective advantage.

The fruits of most of the 60 species of *Elaeocarpus*, a genus of trees native to the Asian tropics and Australasia, are blue[8]. Those of *E. angustifolius* (syn. *E. sphaericus* and *E. grandis*) produce a particularly brilliant colour, but no pigments can be extracted with acidic methanol. E. J. H. Corner wrote[9] that "the blue colour of the cuticle is caused, not by a blue pigment, but by the structure of the cuticle which reflects blue light". The colour is clearly limited to the epidermis of the fruit and is not removed by contact with water, indicating that the structural basis is in the cell layer[10,11]. Diffuse reflectance measurements of the fruit surface (Fig. 1) peak at 439 ± 2 nm (s.e.m.; $n = 5$). Because the colour is uniform at different angles, and reflectance does not increase at shorter wavelengths, both diffraction and Tyndall scattering can be excluded as the basis of colour production[1]. Assuming a refractive index of 1.35–1.45 for the hypothetical structure[12], the thickness of layers responsible for colour production can be predicted using the standard formula for thin-film interference[13]: thickness $= \lambda/4\mu \cos\theta$ where θ is refracted angle of light in the filter, μ the refractive index of the film, and λ the peak wavelength for constructive interference. This equation predicts a thickness of 76–81 nm, assuming the refractive index of the filter is greater than the surrounding medium (otherwise the thickness would be twice that predicted).

Light (Fig. 2*a*) and transmission electron microscopy (Fig. 2*b–d*) reveal a remarkable structure beneath the outer cell walls of the adaxial epidermis. This structure, termed an iridosome (based on analogous structures in animals[1]), consists of a roughly parallel network of electron-translucent strands each 78 ± 4 nm thick ($n = 5$; each value is the mean of 10 measurements within an iridosome of each fruit). Strands are separated by lacunae of 39 ± 5 nm, and paradermal sections of the iridosome (Fig. 2*d*) reveal straight rows (62 ± 3 nm wide and 62 ±

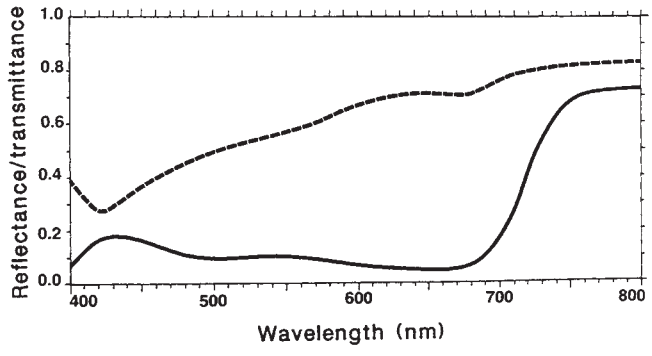

FIG. 1 Optical properties of the iridescent blue fruits. Fruits were collected from two trees at the USDA National Clonal Germ Plasm Collection in Miami. Diffuse reflectance of the intact fruit wall (compared to an optically white barium sulphate surface) was measured with a Li-Cor 1800 spectroradiometer attached by a fibre optic probe to an integrating sphere (Li-Cor Instruments, Lincoln, Nebraska 68504). Transmission through the epidermis was measured by the spectroradiometer attached via a fibre-optic probe to the photographic tube of a Leitz dialux microscope using the ×40 objective (transmission in the absence of tissue was divided into the scan). Dotted line, transmittance; solid line, reflectance.

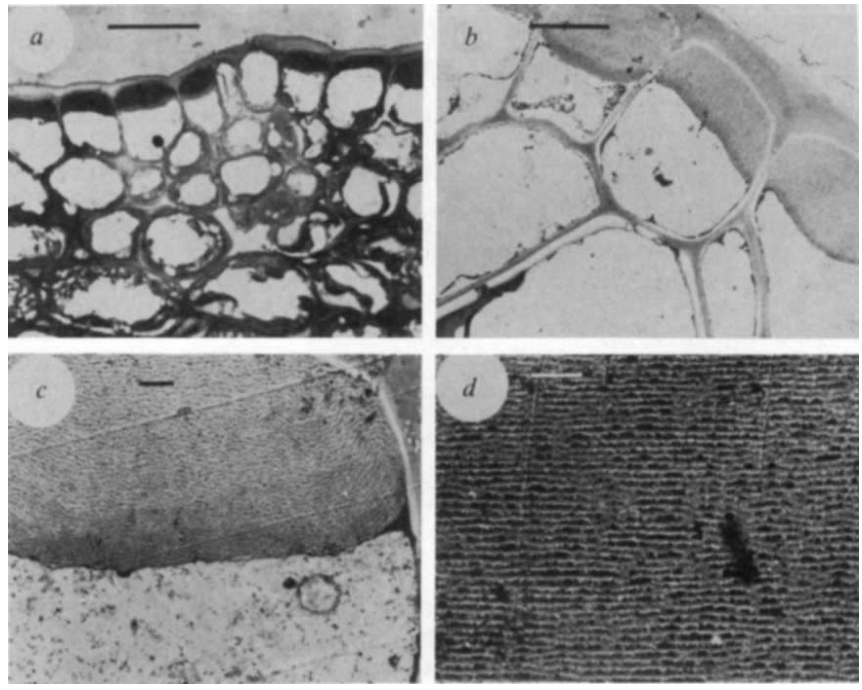

FIG. 2 Micrographs of fruit tissue, showing the location and structure of the iridosome. *a*, Light micrograph of tissue (1-μm thick, stained with toluidine blue. Iridosomes are located immediately beneath the epidermal cell walls. Bar, 20 μm. *b–d*, Transmission electron microscopy photographs: *b*, transverse section, layers within the iridosome are clearly seen. Bar, 10 μm. *c*, Detail of the strands in the iridosome. Bar, 1 μm. *d*, Paradermal section of fruit epidermis, showing contiguity of each band. Bar, 1 μm.
METHODS. Fruit tissue was fixed in 3% glutaraldehyde and post-fixed in 1% OsO_4 in 0.1 M cacodylate buffer at pH 7.2. The tissue was dehydrated in an acetone series, embedded in Spurr's low-viscosity resin, and thin sections were cut in a Porter Blum ultramicrotome for microscopy. Grids were stained with lead citrate and uranyl acetate and photographed in a Philips 200 transmission electron microscope. Structures were measured from original negatives using a dissecting microscope and stage micrometer.

3 nm apart). The two views suggest that the iridosome consists of strands organized as a three-dimensional lattice. This structure should intensify colour production, similar to the wing scales of morpho butterflies (*Morpho* sp.)[1,14,15] and the feather barbules of the peacock (*Pavo cristatus* L)[1,16].

The iridisome is not present in the epidermal cells of immature green fruits. In mature fruits it is extracellular, lying between the adaxial wall and the cytoplasmic membrane. The iridosome seems to be secreted by the cytoplasm; its thickness increases with the intensification of blue coloration in the maturing fruits, and the layers next to the cytoplasm are more electron-dense and more closely appressed (Fig. 2, *b*, *c*).

Histochemical staining reveals that the layers of the iridosome consist of polysaccharides, at least partly of cellulose. Iridosomes stain positively for polysaccharides with periodic acid Schiff's reagent[17] and for cellulose with Calcofluor White M2R (ref. 18), and negatively for lignins by the acid phloroglucinol test and for callose by the aniline-blue fluorescence test[19]. The structure is strongly birefringent under polarized light microscopy, suggesting that the polysaccharides are present as linear fibrils.

Iridescent blue may be of selective advantage in the ripe and senescent fruits of *E. angustifolius* in two ways. Although red and black seem to be stronger attractants, 5–7% of the fleshy fruits consumed and dispersed by birds are blue[20]. The fruits of *E. angustifolius* contain a fleshy mesocarp (rich in carbohydrate and protein; E. D. Stiles, unpublished results) surrounding an extremely hard endocarp. They are important in the diets of the cassowary (*Casuarius casuarius*), fruit-eating pigeons and small mammals[21–24]. Not only do the iridescent fruits present a brilliant colour against the green foliage or brown litter on the forest floor, but the colour persists even when the mesocarp is almost completely senescent or has been consumed by beetles.

Photosynthesis in unripe or green ripe fruits contributes greatly to the carbon economy of many plants[25,26]. In fruits producing colour through pigmentation, however, most of the visible wavelengths (400–700 nm) are absorbed by the epidermis except those producing the colour, which are scattered in internal tissues and diffusely reflected[27]. The most brilliantly coloured fruits are those that scatter light most efficiently, such as of *Heliconia*, which have a white unpigmented mesocarp below the blue epidermis. The epidermis (or exocarp) of *E. angustifolius* fruits is transparent at higher wavelengths, where destructive interference occurs (Fig. 1), and should allow the penetration of photosynthetically active radiation above 500 nm to reach the chlorenchymatous tissue in the ripened fruits. The mesocarp of ripened fruits of *E. angustifolius* is relatively rich in chlorophyll (136 ± 37 μg cm^{-2}, $n = 5$; measured according to Arnon[28]), more than the leaves on an area basis but less per unit volume given the 4-mm thickness of this layer[29,30].

I tested the photosynthetic contribution to the carbon economy by measuring carbon dioxide emissions of fruits under field conditions, at 26 °C and 160–175 μmol m^{-2} s^{-1}, 400–700 nm (photosynthetically active radiation, PAR) in diffuse canopy shade of ~8% full sunlight. Fruit-temperature, CO_2 production and PAR were measured beneath a tree crown at Fairchild Tropical Garden, Miami, with a Li-Cor 6000 photosynthesis system. Five ripened fruits were measured simultaneously in a 0.25-l chamber, with 10 repetitions of different combinations of 20 fruits, on 2 days. Fruits were left in darkness for 60 min, their CO_2 emissions measured in the dark, transferred to diffuse shade-light for 60 min, then measured again. Diminished CO_2 production was detected under these low light conditions. Higher PAR levels could not be used because increased fruit temperatures could increase respiration. Fruits exposed to light emitted 9.2 ± 0.2% less CO_2 than those kept in the dark, which respired at 0.28 ± 0.03 mg m^{-2} s^{-1} of CO_2. Fruits were capable of exchanging gases through stomata and lesions developing from the detachment of trichomes. Thus, photosynthesis by ripened and senescing fruits of *E. angustifolius* contributes to the carbon economy of the plant even under shady conditions. □

Received 23 October; accepted 28 November 1990.

1. Fox, D. S. *Animal Structural Colors and Biochromes* (University of California Press, 1978).
2. Gerwick, W. H. & Lang, N. J. *J. Phycol.* **13,** 121–127 (1977).
3. Pederson, M., Roomans, G. M. & Hofsten, A. *Bot. Mar.* **23,** 193–196 (1980).
4. Richards, P. W. *The Tropical Rainforest* (Cambridge University Press, 1952).
5. Fox, D. L. & Wells, J. R. *Am. Fern. J.* **61,** 137–139 (1971).
6. Lee, D. W. *Gard. Bull. Singapore* **30,** 21–29 (1977).
7. Brouillard, R. *Phytochemistry* **22,** 1311–1323 (1983).
8. Coode, M. J. E. *Kew Bull.* **39,** 509–586 (1984).
9. Corner, E. J. H. *Wayside Trees of Malaya* (Government Printing Office, Singapore, 1952).
10. Lee, D. W. & Lowry, J. B. *Nature* **254,** 50–51 (1975).
11. Hébant, C. & Lee, D. W. *Am. J. Bot.* **71,** 216–219 (1984).
12. Woolley, J. T. *Plant Physiol.* **55,** 172–174 (1975).
13. Jenkins, F. A. & White, H. E. *Fundamentals of Optics* (McGraw-Hill, New York, 1957).
14. Anderson, J. F. & Richards, A. G. *J. appl. Phys.* **13,** 748–758 (1942).
15. Lippert, W. and Gentil, K. *Z. Wiss. Mikrosk. Mikrosk. Tech.* **61,** 95–100 (1952).
16. Durrer, H. *Verhandl. Naturf. Ges. Basel* **73,** 204–224 (1962).

17. Jensen, W. A. *Botanical Histochemistry* (Freeman, San Francisco, 1962).
18. Dodds, J. H. & Roberts, L. W. *Experiments in Plant Tissue Culture* 2nd ed (Cambridge University Press, New York, 1985).
19. Gahan, P. B. *Plant Histochemistry and Cytochemistry* (Academic, New York, 1984).
20. Wheelwright, N. T. & Janson, C. H. *Am. Nat.* **126,** 777–799 (1985).
21. Crome, F. H. J. *Emu* **76,** 8–14 (1976).
22. Frith, H. J., Crome, F. H. J. & Wolfe, T. O. *Emu* **76,** 49–58 (1976).
23. Stocker, G. C. & Irvine, A. K. *Biotropica* **15,** 170–176 (1983).
24. Pratt, T. K. & Stiles, E. D. *Biotropica* **17,** 314–321 (1985).
25. Bazzaz, F. A., Carlson, R. W. & Harper, J. L. *Nature* **279,** 554–555 (1979).
26. Blanke, M. M. & Lenz, F. *Plant Cell Env.* **12,** 31–46 (1989).
27. Kay, Q. O. N., Daoud, H. S. & Stirton, C. H. *Bot. J. Linn. Soc.* **83,** 57–84 (1981).
28. Arnon, D. I. *Pl. Physiol.* **24,** 1–15 (1949).
29. Björkman, O. in *Physiological Plant Ecology I, Encyclopedia of Plant Physiology* Ser. 2, 57–107 (Springer, Heidelberg, 1981).
30. Lee, D. W., Bone, R. A., Tarsis, S. & Storch, D. *Am. J. Bot.* **77,** 370–380 (1990).

ACKNOWLEDGEMENTS. I thank G. Chidvilasanda, A. Zuniga, E. D. Stiles, J. Richards, J. Fisher, G. Valcarce and M. Upright. Supported by the American Philosophical Society.

A Cu(I)-semiquinone state in substrate-reduced amine oxidases

David M. Dooley*, Michele A. McGuirl*, Doreen E. Brown*, Petra N. Turowski*, William S. McIntire† & Peter F. Knowles‡

* Department of Chemistry, Amherst College, Amherst, Massachusetts 01002, USA
† Department of Molecular Biology, Veterans Administration Medical Center, San Francisco, California 94121, USA
‡ Department of Biochemistry and Biophysics, Leeds University, Leeds LS2 9JT, UK

THE role of copper in copper-containing amine oxidases has long been a source of debate and uncertainty[1]. Numerous electron paramagnetic resonance (EPR) experiments[2–6], including rapid freeze-quench studies[7], have failed to detect changes in the copper oxidation state in the presence of substrate amines. One suggestion that copper reduction might occur[8], has never been confirmed. Copper amine oxidases contain another cofactor, recently identified as 6-hydroxydopa quinone (topa quinone)[9], which is reduced by substrates. Copper has been implicated in the reoxidation of the substrate-reduced enzyme[10–12], but the failure to detect any copper redox change has led to proposals that Cu(II) acts as a Lewis acid[13], that it has an indirect role in catalysis[14], or that it serves a structural role[6]. We present evidence for the generation of a Cu(I)-semiquinone state by substrate reduction of several amine oxidases under anaerobic conditions, and suggest that the Cu(I)-semiquinone may be the catalytic intermediate that reacts directly with oxygen.

EPR spectral changes accompanying the addition of an appropriate amine to several amine oxidases under anaerobic conditions are shown in Fig. 1. In each case, a relatively sharp signal at $g \sim 2$ is observed, although the yield of this species is variable. Scans of the $g \sim 2$ signal at higher resolution (Fig. 2) show that the same radical is formed in different amine oxidases. Because the radical EPR spectrum is independent of the enzyme and substrate used, the radical must be associated with a moiety that is conserved among the amine oxidases examined. The spectra in Fig. 2*a* are essentially identical to the EPR spectra of amine oxidases that had been anaerobically reduced in the presence of cyanide or *t*-butylisocyanide (refs 5, 10, 15); these ligands are thought to trap the semiquinone form by stabilizing Cu(I). Addition of cyanide to reduced porcine plasma amine oxidase dramatically increases the intensity of the weak $g \sim 2$ signal (evident in Fig. 1), thereby allowing the characteristic hyperfine structure to be resolved (Fig. 2*b*). The assignment of the $g \sim 2$ signal to a semiquinone radical is supported by a variety of evidence[10,15], including pulsed-EPR studies (J. McCracken, J. Peisach and D.M.D., manuscript in preparation).

Double integration indicates that the yield of the semiquinone in the absence of cyanide ranges from <1% (porcine plasma amine oxidase) to ~20% (pea seedling diamine oxidase and *Arthrobacter* P1 methylamine oxidase) of the theoretical maximum, calculated from the enzyme concentration and assuming a 1:2 protein:quinone stoichiometry[10,16].

Two independent methods were used to quantitate the Cu(II) EPR signal in the substrate-reduced forms of pea seedling diamine oxidase and *Arthrobacter* methylamine oxidase. Vänngård has shown that the area of the $M_I = -3/2$ hyperfine line in a first-derivative Cu(II) EPR spectrum is proportional to the total intensity[17]; comparison of these peak areas for the resting and substrate-reduced enzymes, obtained under identical conditions, indicates that ~40% of the Cu(II) is reduced. Alternatively, the contribution of the sharp $g \sim 2$ signal was mathematically subtracted from the EPR absorption envelope, which was then integrated to give the Cu(II) intensity. Again using the resting enzyme as a standard, the results were in good agreement with those obtained from the integration of the lowest hyperfine line. A lower yield of the semiquinone, relative to the

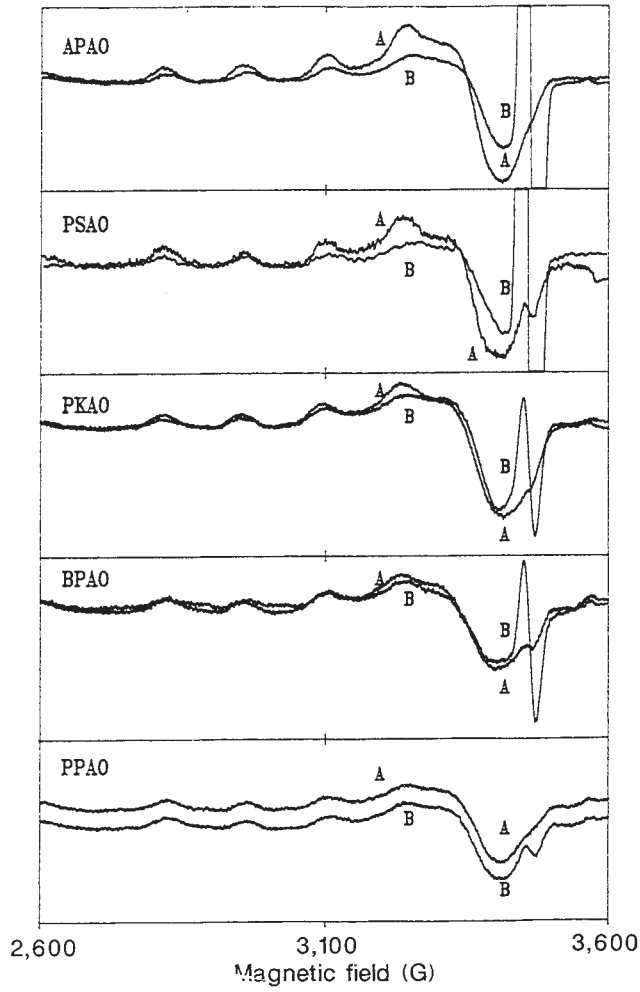

FIG. 1 Room-temperature EPR spectra of amine oxidases from *Arthrobacter* P1 (APAO), pea seedling (PSAO), porcine kidney (PKAO), bovine plasma (BPAO) and porcine plasma (PPAO), before (A) and after (B) anaerobic addition of substrate. Spectra were obtained in 0.3 mm × 6 mm × 100 mm glass microslides (Vitro Dynamics) on a Bruker 220D SRC instrument immediately after samples were prepared and sealed in a nitrogen atmosphere glove box. Frequency, 9.8 GHz; power, 20 mW; modulation amplitude, 20 G; [enzyme], 0.3–0.8 mM in 50 mM barbital, pH 8.0 (APAO, BPAO, PPAO), 50 mM PIPES, pH 7.0 (PSAO), or 0.1 M phosphate, pH 7.2 (PKAO); [substrate], 1–3 mM benzylamine (APAO, BPAO, PPAO) or cadaverine (PSAO, PKAO). The PPAO spectra are offset for clarity.